Hindawi
Geofluids
Volume 2022, Article ID 9433757, 12 pages
https://doi.org/10.1155/2022/9433757

Research Article

Research on Sound Source Material Recognition Technology in Indoor Geotechnical Inspection

Huajie Guo,[1] **Huihuang Jiang**,[1,2] **and Mingxian Gao**[2]

[1]*Postgraduate Department, China Academy of Railway Sciences, Beijing 100081, China*
[2]*China Academy of Railway Sciences (Shenzhen) Research and Design Institute Co., Ltd, Shenzhen 518057, China*

Correspondence should be addressed to Huajie Guo; guohuajie.765@163.com

Received 19 March 2022; Revised 14 May 2022; Accepted 27 May 2022; Published 29 June 2022

Academic Editor: Guang-Liang Feng

Studies have shown that physical parameters such as size have obvious influence and relevance on the sound spectrum structure. In order to study the new detection technology of sound recognition of compaction of soil, this article conducted a large number of indoor soil sample hammering tests. The timbre features of the sound are extracted by the impact sound feature extraction method based on the principle of auditory perception, and the focus is on the correlation between frequency domain eigenvalues such as spectral centroid and different compaction of soil. By grouping and analyzing the multiple sets of acoustic samples after the different compaction of soil samples are excited, we found that the centroid feature of the subband spectrum can well represent the compaction of soil, and the two have a strong correlation; the maximum correlation coefficient is up to 0.81. The research results show that when the reasonable hammering force range of exciting soil is 30 N~89 N, the subband spectrum centroid feature is used as an index to characterize the compaction of soil, which can be used to infer the compaction of soil.

1. Introduction

In recent years, the object has been identified in reverse by collecting the sound emitted by an object that excites a certain structure and extracting its characteristic parameters. It is to find out the physical properties of the sound source from the sound. This "reverse research" sound source material identification technology has received a lot of attention. Sound classification as an in-depth study of pattern recognition problems has begun to appear in recent years [1–6]. When a certain structure is excited, the impact sound includes a lot of information related to the characteristic attributes of the structure. It is similar to microseismic and acoustic emission signals, which contain a large amount of rock fracture information [7–9]. Diezma-lglesias et al. used acoustic timbre characteristics to detect the degree of hollowness of watermelon, which can determine the ripeness of watermelon [10, 11]. The tone characteristics are timbre. Tone recognition is widely used, such as Burred et al. who performed instrument recognition based on accurate timbre models [12]. Automatic sound source target recognition technology through timbre has been widely used in military and civilian fields. For example, Ke'an of Northwestern Polytechnical University and others have made certain progress in the application of timbre for underwater target recognition according to the characteristics of human hearing and determined the timbre model. At the same time, three-dimensional and five-dimensional tone space combined with statistical analysis methods are used to distinguish traffic intersection noise and underwater noise, and the practical application has been successful [13–17].

Liang et al. [18] applied a dissimilarity evaluation experiment and MDS analysis method to study three kinds of impact sound signals of aluminum plate, linden wood laminate, and PVC plate, from spectral characteristics, auditory perception characteristics, and FrMFCC (signal characteristics extracted based on STFT transformation) researched on characteristics. Combining the correlation analysis of the physical parameters of the material, it is concluded that the classification effect of auditory perception features (such as the centroid of the spectrum) reaches more than 65%, and the classification effect of the sound source is good, and the

Table 1: Physical parameter and mechanical indexes of soil samples.

Soil sample number	Moisture content (%)	Soil mass (g)	Wet density ($g{\cdot}mm^{-3}$)	Dry density ($g{\cdot}mm^{-3}$)	Void ratio	Compaction (heavy compaction) (%)	Element
T1	6	1650	1.65×10^{-3}	1.47×10^{-3}	0.49	76.6	Granite residual soil (silt sand)
T2	6	1730	1.74×10^{-3}	1.54×10^{-3}	0.42	80.3	
T3	6	1800	1.81×10^{-3}	1.6×10^{-3}	0.36	83.5	
T4	6	1880	1.89×10^{-3}	1.68×10^{-3}	0.31	87.2	
T5	6	1940	1.95×10^{-3}	1.73×10^{-3}	0.27	90.0	
T6	6	1990	2×10^{-3}	1.77×10^{-3}	0.23	92.3	
T7	6	2050	2.06×10^{-3}	1.83×10^{-3}	0.20	95.1	
T8	6	2110	2.12×10^{-3}	1.88×10^{-3}	0.16	97.9	
T9	6	2155	2.16×10^{-3}	1.92×10^{-3}	0.14	100.0	

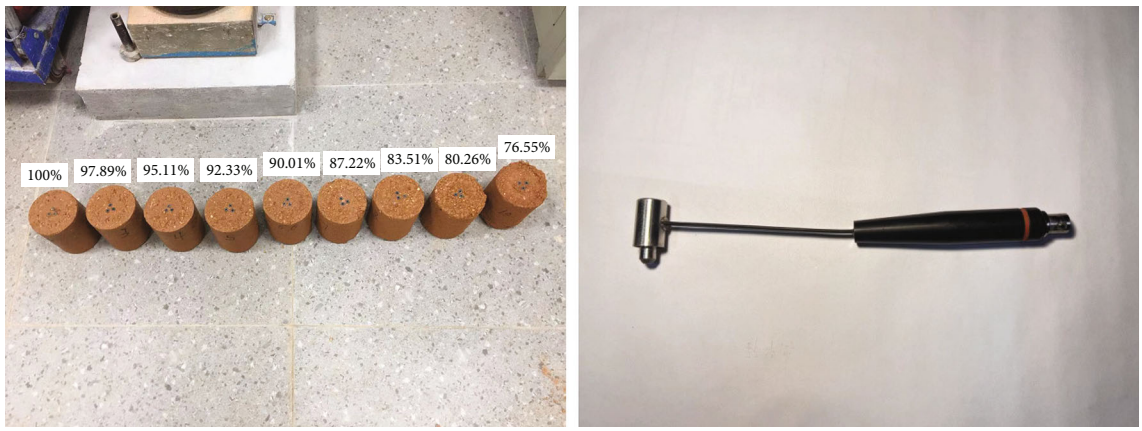

Figure 1: Hammering diagram of indoor soil sample and force hammer.

noise resistance is strong. Kai et al. have studied ground type recognition when crawler robots are walking in geotechnical engineering [19], Ozkul et al. recognize the walking sound of a hexapod robot based on the nonmodel chromatographic band energy and vector time, and the recognition process is not disturbed by environmental and mechanical noise [20]. At present, the principle of the detection methods of railway subgrade compaction at home and abroad is based on the vertical response acceleration of the vibrating wheel of the roller, in addition to the traditional detection technology (ring knife method, sand filling method, and nuclear densitometer method). It reflects the degree of soil compaction through the response of the vibrating wheel. Zhang et al. used the sound generated by the excitement of the steel wheel of the roller in the harmonic ratio to characterize the degree of compaction of the soil but only conducted exploration for the backfill with a particle size of 400 mm or more [21]. Glowacz et al. select the single-phase asynchronous motor as the research object; propose a frequency-based feature extraction method for the sound of the motor during operation, bearing fault, and winding coil short-circuit fault; and optimize the classification with the nearest average classifier [22]. Glowacz extracts features by calculating spectral differences for the sounds emitted by the four operating states of a three-phase asynchronous motor [23]. Prawin proposes a new two-stage damage diagnostic technique for breathing crack identification in using improved mel-frequency cepstral analysis. First, the measured acceleration time history responses are converted into mel-frequency cepstral coefficients using improved mel-frequency cepstral analysis. The improved mel-frequency cepstral coefficients of the healthy structure and the structure with localized damage correspond to different mel-frequency cepstral analyses. Second, the spatial location of the breathing crack is established through offline monitoring, by exciting the structure with bitone harmonic excitation. Finally, experimental investigations have been carried out to demonstrate that the proposed damage diagnostic approach is capable of detecting and localizing multiple and also subtle cracks [24].

In the process of vibrating and rolling the railway subgrade roller, the sound collection is greatly affected by the machine's own engine and the working machinery in the environment. It is difficult to analyze the degree of soil compaction with the collected sound tone. Therefore, this article firstly analyzes the sound of different compaction

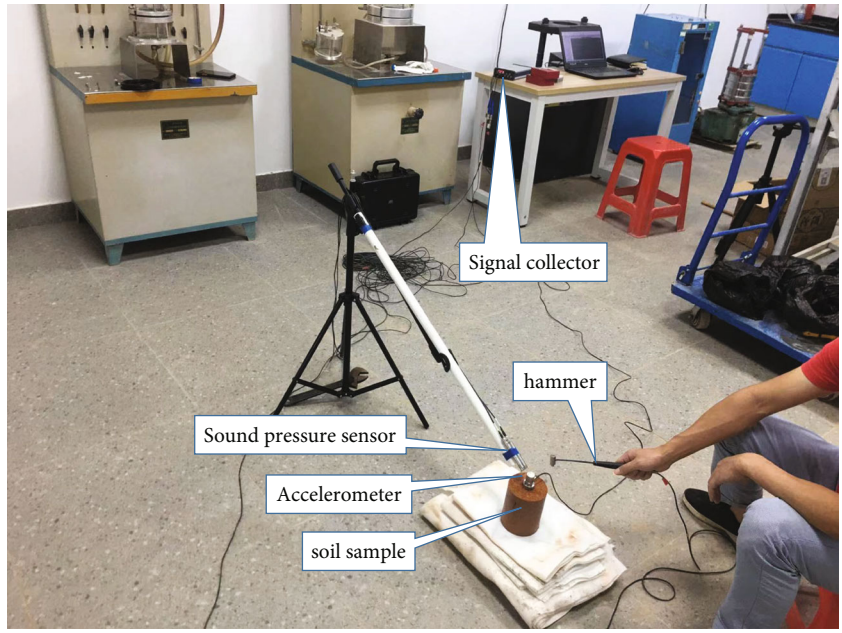

Figure 2: Hammering process.

Table 2: Soil sample hammering schedule.

Soil sample	Plan hammering force (N)	Measured hammering force (N)	Number of hammers	Acoustic signal sample number	Sampling frequency (Hz)
T1	35, 45, 55, 65, 75, and 85 A total of six levels	32~58	40-50 times per soil sample	1~56	51200
T2		19~64		57~104	
T3		23~78		105~153	
T4		38~84		154~204	
T5		48~90		205~247	
T6		35~94		248~295	
T7		30~128		296~338	
T8		41~153		339~377	
T9		55~196		378~434	

soil samples in the room after hammering and identifies soils with different compaction degrees. It is hoped that through research, the sound frequency spectrum characteristic value that can characterize the degree of soil compaction and the sound source material identification method for judging the degree of soil compaction can be obtained.

2. Soil Sample Preparation and Sound Acquisition

2.1. Test Soil Sample Preparation. In order to study the applicability and application operation methods of sound source material identification technology on the road roller during the rolling process of roadbed soil, this article takes the commonly used roadbed filler-granite residual soil in Guangdong as the object. Starting from the hammering sound of indoor soil samples, this paper explores the influence of different soil densities (corresponding to the compaction degree of subgrade soil) on the timbre of hammering sound and seeks to characterize the soil spectrum structure of body density and characteristic value. The fine particle content of common granite residual soil is about 30%, and the optimal moisture content when used as a filler is 6%. In this paper, nine cylindrical soil samples with the same geometrical dimensions were made indoors by the conventional compaction method (Highway Geotechnical Test Regulations JTG 3430-2020). The diameter and height are 100 mm and 117 mm, the volume is 997000 mm^3, and the water content is 6%. The dry density is compared with the maximum dry density obtained in the standard compaction test, and the compaction of each soil sample is converted into 76.6%, 80.3%, 83.5%, 87.2%, 90.0%, 92.3%, 95.1%, 97.9%, and 100.0%. The degree of compaction is the ratio of the dry density of the existing soil sample to the maximum dry compaction in the room. Physical parameter and mechanical indicators of soil samples are described in Table 1.

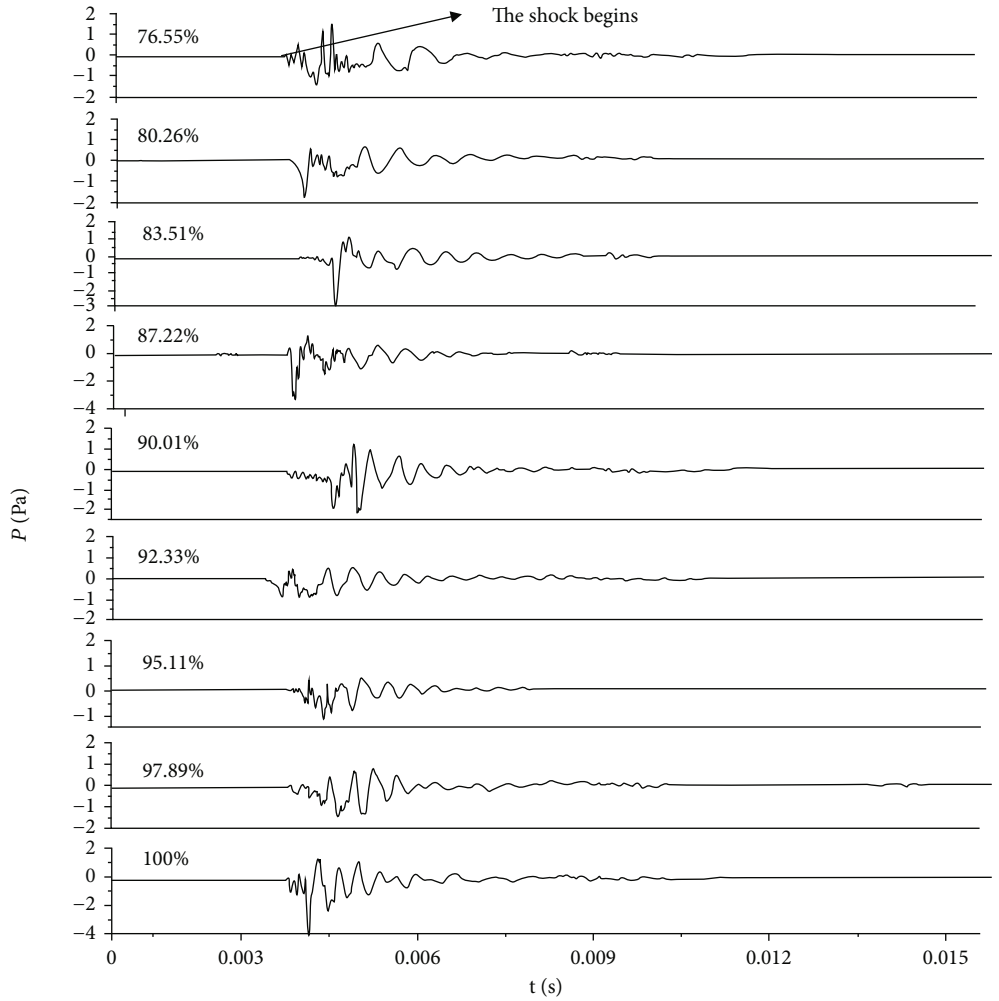

Figure 3: Time-domain diagram of sound information of hammering soil samples.

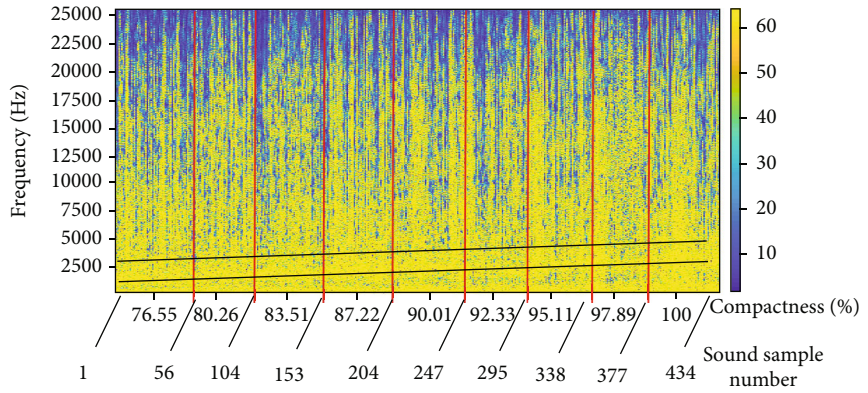

Figure 4: Full-band spectrograms of sound samples of different compaction of soil samples (yellow represents the peak frequency response).

2.2. Hammering Method and Sound Acquisition. In the process of hammering the soil sample, in order to obtain stable, accurate, reliable, and effective hammering sound information, the test plan focuses on the experimental environment, force hammer (material, hammering force, and hammering method), sound pressure sensor (using frequency, sensitivity), and the layout of the sound pressure sensor.

Environment: in order to avoid external noise interference, the test is carried out in an echo-free and noise-free geotechnical room after 23 o'clock, and the sound is

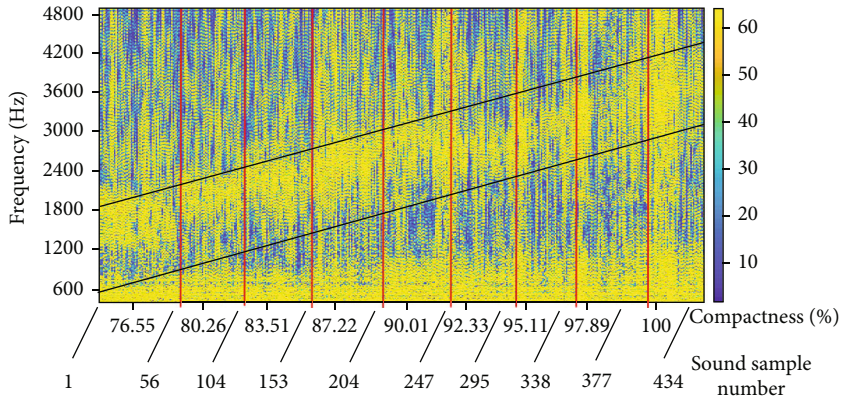

Figure 5: Spectrogram of soil samples with different compaction of soil samples after frequency reduction by one-sixth.

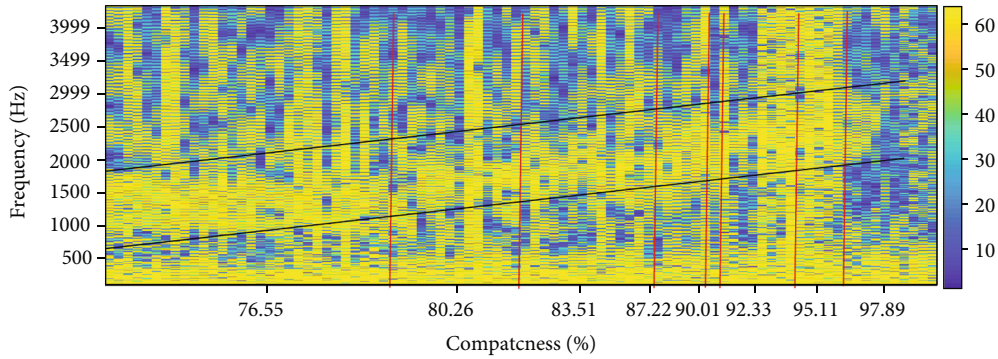

Figure 6: Frequency spectrum after 35(L) N hammering force is reduced by one-sixth.

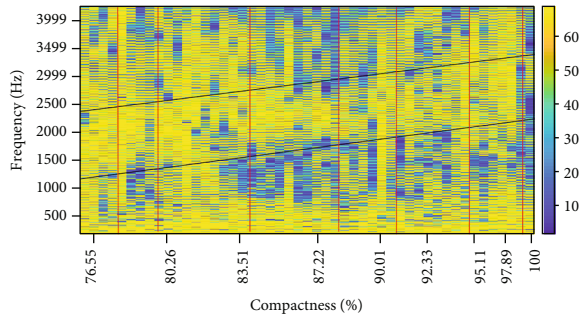

Figure 7: Frequency spectrum after 45(L) N hammering force is reduced by one-sixth.

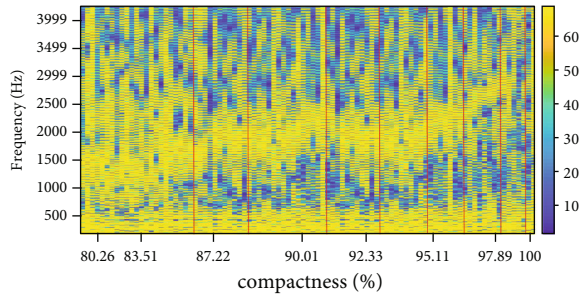

Figure 8: Frequency spectrum after 55(L) N hammering force is reduced by one-sixth.

collected in time after the soil sample is made in the geotechnical room to avoid test errors caused by the evaporation of soil moisture.

Force hammer: the force hammer is Oriental Institute INV9310 (ICP) small force hammer with a range of 500 N. The force hammer is shown in Figure 1.

Instruments and sensors: the sound wave acquisition and analysis instrument of the Oriental Institute NV3602-C2 (L) and the INV9206 series sound pressure sensor are used to collect the sound after hammering.

Test installation: put the soil sample on the geotextile, install the sound pressure sensor with a tripod, and aim at the center of the soil sample. The soil samples are shown in Figure 1. The experiment process is shown in Figure 2.

Hammering scheme: in order to facilitate the classification of the hammering force, by installing a pressure sensor and a gain amplifier inside the hammer, during the hammering process, the hammering force acting on the soil sample was measured. The plan is to carry out the hammering test with six levels of hammering force of 35 N, 45 N, 55 N, 65 N, 75 N, and 85 N, and hammer the surrounding soil samples with force. Avoid hammering the sensor during hammering; at the same time, the hammering point should be as close as possible to the periphery of the soil at the same distance from the center, and avoid repeated hammering at the same hammering point. Taking the center of the soil sample as the circle point, use a black pen to draw a diameter of 80 mm The circle on which the hammer is hammered

Table 3: Statistical table of correlation analysis between different compaction of soil samples and subband spectral centroid under different hammering forces.

Serial number	Plan hammering force (N)	Measured hammering force (N)	Soil compaction (%)	Correlation equation	Correlation coefficient	Subband spectrum centroid (Hz)
1	35	35(L)	76.6~97.9	$y = 45x - 1508$	0.61	1519~3018
2	45	45(L)	76.6~100	$y = 32x - 518$	0.67	1518~3038
3	55	55(L)	76.6~100	$y = 41x - 1279$	0.81	1657~2920
4	65	65(L)	80.3~100	$y = 39x - 1136$	0.71	1723~3115
5	75	75(L)	83.5~100	$y = 37x - 933$	0.67	2118~3040
6	85	85(L)	87.2~100	$y = 32x - 336$	0.58	2031~3127

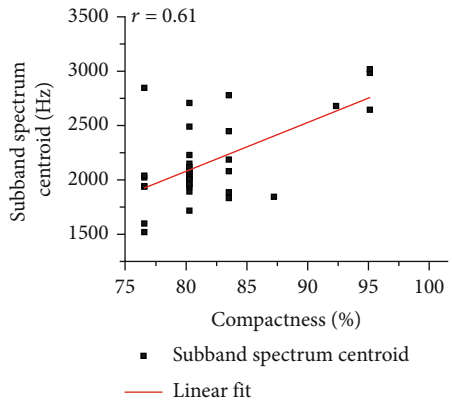

Figure 9: Correlation graphs of soil samples with different compaction degrees under the action of 35(L) N hammering force and the centroid of sound subband spectrum.

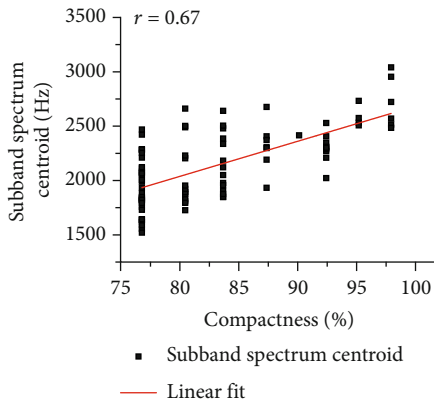

Figure 10: Correlation graphs of soil samples with different compaction degrees under the action of 45(L) N hammering force and the centroid of sound subband spectrum.

ensures that the acoustic sample is not affected by the position of the hammer. During the test, try to have the same hammering force each time, and the hammering direction is perpendicular to the upper surface of the soil sample. In the test process, when the iron hammer is used for the force hammer, the sound difference of the soil samples with different compaction degrees is very different when they are excited. The sound obtained by hammering soil samples with different compaction degrees is very different. When the hammering force is greater than 90 N, the hammering is likely to cause potholes and damage to the surface of T1~T4 soil samples with a degree of compaction less than 90%. Therefore, during the test, the hammer must be controlled and the hammering force cannot be greater than 90 N. The specific hammering and signal acquisition plan are shown in Table 2.

In the experiment, 40-50 sound samples were collected for each compaction soil sample after hammering, a total of 434 sound samples. In the experiment, the sampling frequency $F_s = 51200$ Hz. As shown in Table 2 hammer plan, during the test, the main hammering force measured was concentrated in the range of 30 N~100 N. In order to simplify the problem and facilitate analysis, the impact force of each level is included in the same level within the range of ±5 N for statistical analysis, namely, 30 N~39 N, 40 N~49 N, 50 N~59 N, 60 N~69 N, 70 N~79 N, and 80 N~89 N. In the following, these six force levels are, respectively, expressed as 35(L) N, 45(L) N, 55(L) N, 65(L) N, 75(L) N, and 85(L) N, excluding individual hammering forces greater than 90 N sound samples.

2.3. Basic Characteristics of the Sound Signal of Soil Sample Hammering. Feature extraction stage: first, segment the sound of the continuous excitation soil sample into the sound of a single excitation soil sample, and ensure that the excitation moment is included in each hit sound sample after segmentation. The measured excitation instant duration is about 5 ms. After multiple data analysis and processing, it is obtained that a sound sample with a duration of 256 points forward from the excitation moment and a duration of 0.6 s is intercepted in a single excitation sound signal, which can completely include the excitation sound moment and the sound wave attenuation section to ensure the integrity and validity of data analysis. Feature extraction is performed on the sound samples after each hammer hits the soil; due to the impact of hammer height, force hammer, and human subjective control, it is impossible to achieve the same magnitude of hammering force. Therefore, for each compaction soil sample, each 10 N is a hammering power level to a group, and the different compaction soils and timbre characteristics are normalized and analyzed within each hammering power level. Take the average value of timbre

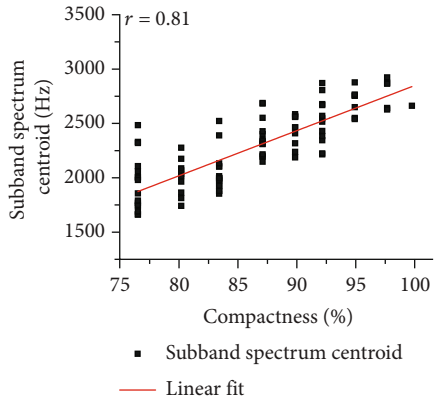

Figure 11: Correlation graphs of soil samples with different compaction degrees under the action of 55(L) N hammering force and the centroid of sound subband spectrum.

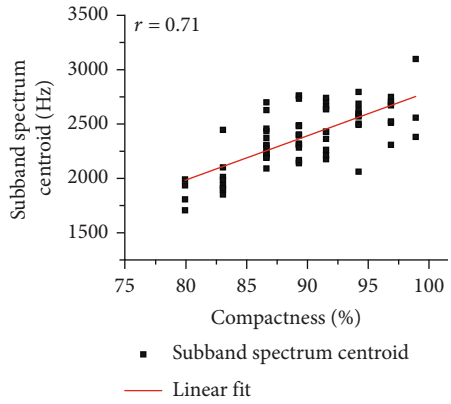

Figure 12: Correlation graphs of soil samples with different compaction degrees under the action of 65(L) N hammering force and the centroid of sound subband spectrum.

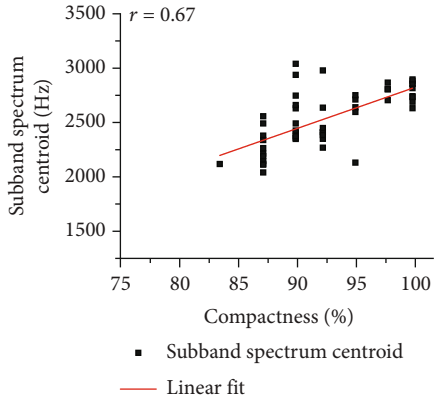

Figure 13: Correlation graphs of soil samples with different compaction degrees under the action of 75(L) N hammering force and the centroid of sound subband spectrum.

characteristics of each soil sample in different hammering strength levels at 10 N intervals, and then, perform normalization analysis with the degree of soil compaction again to obtain an accurate timbre characteristic quantity that can characterize the degree of soil compaction.

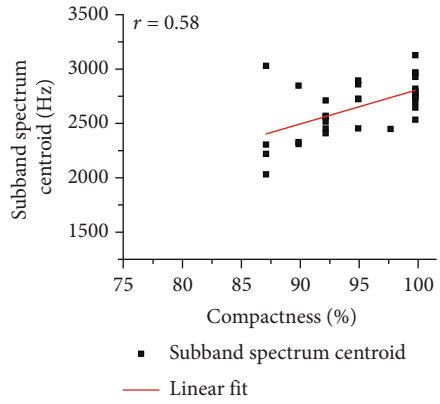

Figure 14: Correlation graphs of soil samples with different compaction degrees under the action of 85(L) N hammering force and the centroid of sound subband spectrum.

Figure 3 shows the time-domain diagram of nine soil samples with a compaction degree of 76.6%-100% under the same hammering force (50 N). The duration of sound pressure amplitude attenuation to 0.2 Pa is about 15 ms, and the change is obvious. The 0.015 s time-domain diagram of nine sound samples including the moment of excitation is analyzed as follows: the sound wave waveform is obvious when the soil sample is excited, and during the field test, the soil samples with different compaction degrees can be distinguished by the human ear during the hammering process, so the spectrogram and timbre characteristics can be used for further analysis.

3. Analysis and Selection of Hammering Sound Timbre Characteristics

In the field of nonverbal target sound source recognition, target recognition based on human ears is the most direct and effective method. The manifestation of sound is the change of sound pressure. The basic parameters describing changes in sound pressure are amplitude, frequency, and phase. Sound source recognition is the study of the perception and discrimination of these parameters by the human ear auditory system, that is, the perception of the human ear on the loudness and pitch of the sound. In order to improve the recognition rate of the human ear to the sound source target, it is necessary to train the human ear. At the same time, the subjective evaluation test is used to identify the target from the perspective of timbre characteristics, that is, the psychoacoustics in auditory perception. In addition to loudness and pitch, psychoacoustics also uses timbre characteristics to describe sounds. The timbre has multidimensional properties, and its decisive factors are the onset time, the spectral centroid, and the fine structure of the frequency spectrum. In order to achieve a better identification effect, through subjective evaluation, regression analysis, statistical analysis, and multidimensional scaling analysis (MDS), select appropriate timbre characteristics, reduce and quantify their dimensions, establish a timbre model that can reflect subjective feelings, and finally verify the timbre model and characteristics to improve the target recognition effect. The spectral centroid feature is obtained in this way.

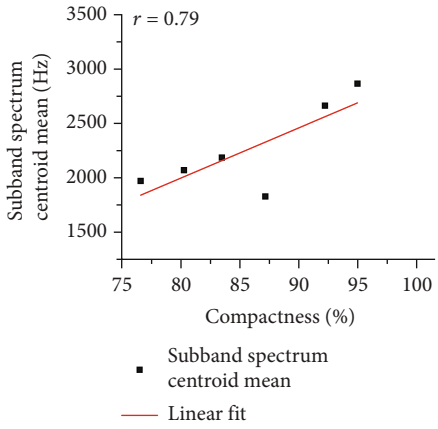

Figure 15: Correlation diagram of the mean value of the centroid of the subband spectrum and the soil mass with different compaction degrees under the action of 35(L) N hammering force.

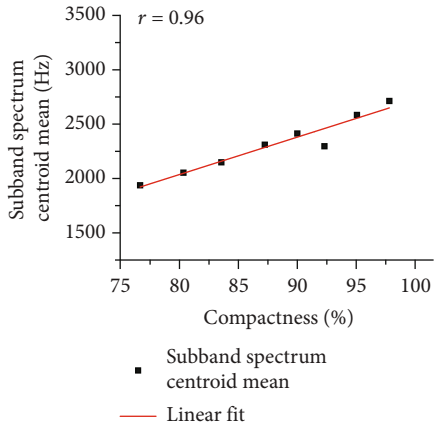

Figure 16: Correlation diagram of the mean value of the centroid of the subband spectrum and the soil mass with different compaction degrees under the action of 45(L) N hammering force.

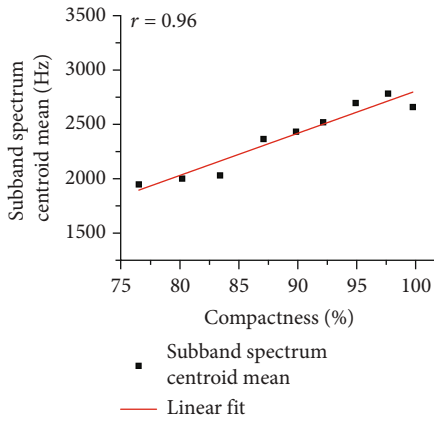

Figure 17: Correlation diagram of the mean value of the centroid of the subband spectrum and the soil mass with different compaction degrees under the action of 55(L) N hammering force.

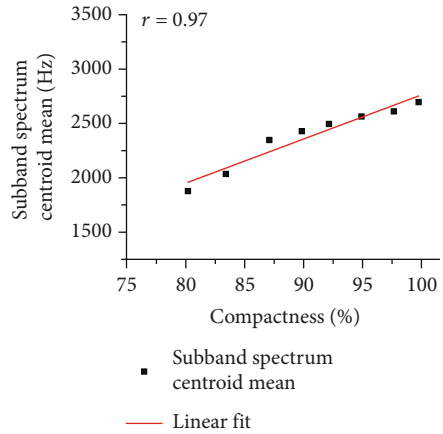

Figure 18: Correlation diagram of the mean value of the centroid of the subband spectrum and the soil mass with different compaction degrees under the action of 65(L) N hammering force.

3.1. Timbre Characteristic Analysis Method of Hammering Sound. When extracting features of impact sound used for sound source identification, consider the four physical parameters of the material: damping, density, Young's modulus, and Poisson's ratio, and from the three signal conversion methods of the time-domain envelope and characteristic and spectral structure (FFT), the signals of metal, wood, and polymer can be clearly distinguished, such as the time-domain centroid, rising slope, and decay slope in the time-domain feature and the spectral centroid, spectral slope, cepstral coefficient, etc., in the spectral feature. Linear regression analysis is performed on these extracted features with variables affecting the auditory perception space, resulting in a linear representation of each feature [14].

This paper analyzes the sound samples collected in the experiment with the characteristics of timbre and the frequency spectrum structure after frequency reduction. When analyzing the relationship between timbre characteristics and compaction, firstly, intercept each impact sound sample, the length is 1~2 s, and the sampling frequency is 51200 Hz. In view of the short duration of the impact sound of the soil, in order to ensure the integrity of the analysis results, take each sound sample forward 256 points from the starting point of excitation as the starting point of analysis. Use matlab to automatically identify the starting point, and calculate the minimum, average, and maximum of each tone feature, a total of 192-dimensional tone features. Among them, mfcc (mel-frequency cepstrum coefficient), dmfcc (first-order differential mel-frequency cepstral coefficient), and ddmfcc (second-order differential mel-frequency cepstral coefficient) each has 36 dimensions. Perform correlation analysis between the calculation results of each feature and different compaction degrees to obtain the correlation coefficient. Take the characteristic value with a correlation coefficient greater than 0.75, and do a normalization analysis with different compaction degrees of the soil to obtain the normalized equation, which can be used as the basis for reverse predicting the compaction degree of the soil. When analyzing the relationship between the spectral structure of the sound sample and the degree of compaction, for the

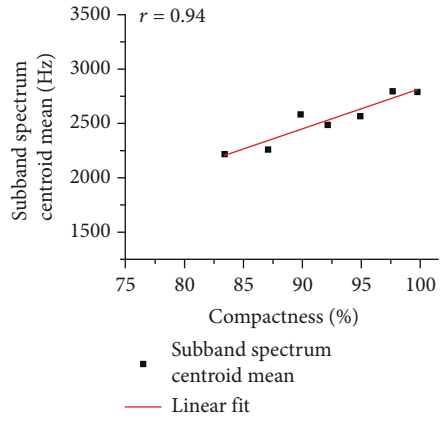

Figure 19: Correlation diagram of the mean value of the centroid of the subband spectrum and the soil mass with different compaction degrees under the action of 75(L) N hammering force.

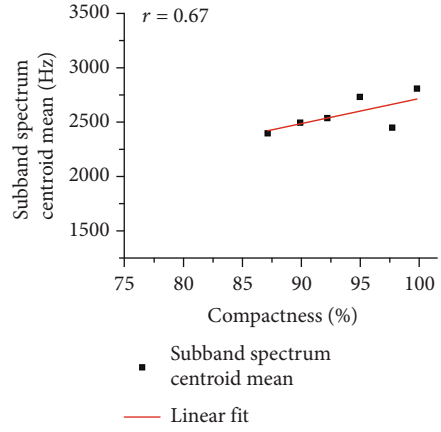

Figure 20: Correlation diagram of the mean value of the centroid of the subband spectrum and the soil mass with different compaction degrees under the action of 85(L) N hammering force.

convenience of statistical analysis, take the 1 s duration of the sound sample including the moment of excitation; after performing FFT (Fourier transform) transformation, it is observed that the frequency increases steadily with the increase of compaction in the range of 1 Hz~4000 Hz. In order to further study the rule of this interval and compare it with the original sampling frequency, reduce the sampling frequency by one-sixth. The FFT show that when the sampling frequency is reduced by one-sixth, the main frequency position in the spectrum structure of the soil samples with different compaction degrees does not change much, and the corresponding amplitude increase trend is small, but the high-frequency part has a significant growth trend with the change of compaction degree. Further, use the weighted spectral centroid and subband spectral centroid eigenvalues to calculate. Experiments have proved that the subband spectral centroid feature can distinguish the degree of soil compaction.

3.2. Calculation Method of Eigenvalues of Subband Spectral Centroid. The subband spectral centroid contains information about the frequency distribution and energy distribution of the sound signal. It is one of the parameters describing the properties of the timbre. It mainly represents the center of gravity of the frequency components of the hammering sound and can reflect the characteristics of the fundamental frequency of the main sound waves in the sound signal; the unit is Hz. In the field of subjective perception of hammering sound signals, the subband spectral centroid describes the brightness of the sound. When the sound is dark and deep, the subband spectral centroid is lower, and there are many low-frequency components. When the sound is bright and cheerful, the subband spectral centroid is higher. For high-frequency components. Seo et al. proposed the calculation and analysis method of the subband spectral centroid. When the signal sampling frequency is F_s, the number of sampling points per second is N, the frequency resolution is $\Delta f = F_s/N$, the spectral line is $k = f/\Delta f$, and f is the frequency; when the frequency range is $f_1 \sim f_2$, the corresponding spectral line is $k_1 \sim k_2$; the formula for calculating the subband spectral centroid [25, 26] is as follows (1):

$$f_{sc} = \frac{\sum_{k=k_1}^{k_2} kS(k)}{\sum_{k=k_1}^{k_2} S(k)} = \sum_{k=k_1}^{k_2} k \frac{S(k)}{\sum_{k=k_1}^{k_2} S(k)} = \sum_{k=k_1}^{k_2} k \cdot p(k). \quad (1)$$

The centroid of the subband spectrum is the weighted average frequency within a given frequency band, where $p(k) = S(k)/\sum_{k=k_1}^{k_2} S(k)$ is the ratio of the energy of each spectral line of $k_1 \sim k_2$ to the total energy.

$S(k)$ is the energy spectrum or power spectrum of the signal. That is, the frequency position corresponding to the corresponding spectral line is weighted by the energy ratio, and the weight represents the proportion of each frequency component in the total energy. Using the subband spectral centroid feature can detect the true center position of the signal peak.

4. Characteristic Analysis of Spectral Centroid Characteristic of Soil Sample Density

During the test, collect the sound response under each different hammering force, and use the subband spectral centroid features to analyze and compare the collected sound samples to obtain reasonable characteristic parameters that can characterize the degree of soil compaction.

The full-band spectrogram composed of all 434 sound samples with different compaction degrees in the range of 19 N to 196 N hammering force is shown in Figures 4 and 5. Yellow represents the frequency response peak; that is, there is a harmonic response at this frequency. From the spectrogram in Figure 4, it can be seen that the yellow density of soils with different compaction degrees below 4000 Hz is continuous and the frequency peaks are more concentrated. Therefore, the sound sample with the original sampling frequency of 51200 Hz is reduced to one-sixth of the original sampling frequency to obtain Figure 5. It is found that the frequency band from 1000 Hz to 4200 Hz in Figure 5 obtained after the frequency is reduced by one-sixth has increased steadily.

Table 4: Correlation table between the same level of hammering force and different compaction of soil samples and the subband spectrum centroid mean value.

Serial number	Hammering force (N)	Soil compaction (%)	Correlation equation	Correlation coefficient	Subband spectrum centroid mean (Hz)
1	35(L) N	76.6~ 97.9	$y = 46x - 1646$	0.79	1987~2883
2	45(L) N	76.6~100	$y = 34x - 689$	0.96	1937~2713
3	55(L) N	76.6~100	$y = 38x - 1048$	0.96	1948~2783
4	65(L) N	80.3~100	$y = 40x - 1269$	0.97	1877~2697
5	75(L) N	83.5~100	$y = 37x - 855$	0.94	2118~2790
6	85(L) N	87.2~100	$y = 23x + 428$	0.67	2397~2808

In addition to the acoustic signal spectrogram under all hammering forces, taking the hammering force of 35(L) N as an example, it is found that the spectrogram in this force level range is similar to that in Figure 6. The yellow in each red compartment in Figure 6 represents the spectral peak of each sound sample number corresponding to the compaction soil sample shown on the abscissa. Because the corresponding sound sample number in each hammering force level is not continuous among the 434 sound samples, the sound sample number is not marked.

The results obtained by the hammering force of the other force levels are basically the same as the results of the hammering force of 35(L) N, showing similar laws. Therefore, in summary, there is a band of 1000~4000 Hz that increases with soil compaction in the range of the total hammering force and each level of hammering force. So, reduce the sampling frequency by one-sixth. After reducing the sampling frequency, the band of the spectrogram grows steadily as the degree of compaction increases and is less affected by the hammering force. The frequency spectrum changes at 45(L) N, and 55(L) N levels are shown in Figures 7 and 8, and there are also stable frequency bands from 1000 Hz to 4000 Hz.

Although it is known by common sense that the natural vibration frequency band of soil samples will increase with the increase of its compaction degree, there has been no accurate frequency band range for reference. The sound signal in this experiment is accurately given its frequency band range after FFT transformation, which lays a foundation for the subsequent prediction.

5. Correlation Analysis of the Centroid of the Subband Spectrum That Characterizes the Density of the Soil Sample

5.1. Correlation between the Centroid of Subband Spectrum and the Degree of Compaction of Soil Sample. After performing a one-sixth frequency reduction on the full frequency band spectrum of Figure 4, it is found that there are obvious regular patterns in the range of 1000 Hz to 4000 Hz, as shown in Figure 5. The yellow band in the black wire frame area increases significantly with the increase of soil compaction. This band range was analyzed with the subband spectral centroid and normalized to the same magnitude of the hammer force.

Table 3 lists the specific numerical values and related equations of the subband spectrum centroid feature calculation for soil samples with different compaction degrees in the frequency band of 1000 Hz~4000 Hz under the action of the sixth-level hammer force. The analysis is shown in Figures 9–14. And get the correlation analysis chart.

Figures 9–14 are the correlation analysis diagrams between the soil compaction degree and the subband spectrum centroid eigenvalues under six different hammer strength levels. The correlation coefficients are 0.58~0.81, respectively. Among them, the hammering force corresponding to the nine soil samples under the action of the hammering force of 55(L) N and the characteristic values of the centroid of the subband spectrum extracted by the sound signal are shown in Table 3. The range of spectral centroid is 1657 Hz~2920 Hz, which has the strongest linear correlation with compaction degree, and the correlation coefficient is 0.81.

5.2. Correlation between the Mean Value of the Centroid of Subband Spectrum and the Degree of Compaction of Soil Samples. Under the action of the sixth-level hammer force, the subband spectrum centroid mean and the soil sample compaction degree in the frequency band 1000 Hz~4000 Hz are normalized and analyzed and obtain Figures 15–20 and Table 4.

Analyzing Tables 3 and 4 and Figures 15–20 in the different compaction degree soil samples under the action of six hammering force levels, the correlation coefficient between the corresponding subband spectrum centroid average value and soil compaction degree is 0.67~0.97. Among them, 45(L) N, 55(L) N, 65(L) N, and 75(L) N have a correlation coefficient of 0.94~0.97 at the same level of hammering force, which has a strong correlation. This shows that the subband spectral centroid characteristics extracted from the sound samples collected by hammering soil samples can well reflect the compaction state of the soil, and within this hammering force range, the hammering force has little effect on the correlation between the centroid of the subband spectrum and the degree of compaction. According to the above correlation analysis, when the hammering force is 55(L) N, the correlation coefficients between the subband spectral centroid characteristic value and the soil compaction degree and the subband spectral centroid average value and the soil compaction degree in the six hammering force levels are, respectively, 0.81 and 0.96, showing a strong

correlation. Therefore, when hammering soil in indoor geotechnical testing, the sound can be collected by controlling the hammering force within the range of 55(L) N; the correlation fraction $y = 38x - 1048$ is used to analyze and calculate the centroid characteristics of the subband spectrum and to predict the degree of soil compaction in reverse.

6. Conclusion

Analyzing the spectral centroids and subband spectral centroids of 434 sound samples collected from nine soil samples with different compaction degrees under different hammering forces, we can see that the subband spectral centroids can well represent the degree of soil compaction.

(1) Using spectral centroid analysis of sound samples within the same hammering force level of 45(L) N, 55(L) N, and 65(L) N, the correlation coefficients between the spectral centroid and the different compaction degrees of the soil are 0.39, 0.16, and 0.19, respectively, and the correlation is poor

(2) The spectral centroid and subband spectral centroid characteristics of the sound samples under the same hammering force level and all hammering forces in the range of 30 N to 89 N are analyzed for the correlation with different compaction degrees of the soil. It is found that the centroid feature of the subband spectrum has the strongest correlation with the degree of compaction of the soil, and the correlation coefficient is 0.8, which is almost consistent with the data obtained by the analysis when the hammer force is 55(L) N. It shows that the hammering force has little effect on the centroid of the subband spectrum. The centroid characteristic value of the subband spectrum increases linearly with the increase of soil compaction, which further shows that the centroid characteristic of the subband spectrum can well characterize the soil compaction

(3) After reducing the sampling frequency in the original sound sample spectrogram by one-sixth, it is found that in the range of 1000 Hz to 4200 Hz, the frequency response increases linearly with the increase of compaction. Within the range of 30 N~89 N of hammering force, with every 10 N as a hammering force level, within each hammering force level, use the subband spectral centroid feature to analyze the frequency band of 1200 Hz~4200 Hz to get the law: When the hammering force is 55(L) N, the correlation between the centroid feature of the subband spectrum and the degree of soil compaction is the strongest, with a correlation coefficient of 0.81. The correlation analysis between the mean value of the centroid of the subband spectrum corresponding to each compaction soil sample in the 55(L) N hammering force level and the soil compaction shows that the correlation coefficient is up to 0.96. Using the subband spectrum centroid feature value extracted from the sound collected within the hammering force range of 55(L) N, combined with the correlation equation $y = 38x - 1048$, the degree of soil compaction can be predicted backward

Data Availability

The data used to support the findings of this study are included within the article.

Conflicts of Interest

The authors declare that they have no conflicts of interest.

Acknowledgments

We thank the support and assistance provided by the instruments, equipment, materials, and personnel provided by the Academy of Railway Sciences (Shenzhen) Testing Engineering Co., Ltd. The authors gratefully acknowledge the financial support from the China Academy of Railway Sciences (Shenzhen) Research and Design Institute Co., Ltd under Grant number 2020SZ02. Useful suggestions given by Dr. Tian Xuhua from Northwestern Polytechnical University are also acknowledged.

References

[1] J. C. Brown, "Computer identification of musical instruments using pattern recognition with cepstral coefficients as features," *Journal of the Acoustical Society of America*, vol. 105, no. 3, pp. 1933–1941, 1999.

[2] A. Eronen, "Comparison of features for musical instrument recognition," in *IEEE Workshop on Applications of Signal Processing to Audio and Acoustics*, New Platz, NY, USA, October 2001.

[3] P. Herrera, X. Amatriain, E. Batlle, and X. Serra, "Towards instrument segmentation for music content description: a critical review of instrument classification techniques," in *International Symposium on Music Information Retrieval*, pp. 23–25, Plymouth, Mass, USA, October 2000.

[4] J. Marques and P. J. Moreno, "A study of musical instrument classification using gaussian mixturemodels and support vector machines," Tech. Rep, Cambridge Research Laboratory, Cambridge, Mass, USA, June, 1999.

[5] K. D. Martin, *Sound-source recognition: a theory and computational model, [Ph.D. thesis]*, Massachusetts Institute of Technology, Cambridge, Mass, USA, 1999.

[6] E. Wold, T. Blum, D. Keislar, and J. Wheaten, "Content-based classification search and retrieval of audio," *IEEE Multimedia Magazine*, vol. 3, no. 3, pp. 27–36, 1996.

[7] G. L. Feng, X. T. Feng, B. R. Chen, Y. X. Xiao, and Y. Yu, "A microseismic method for dynamic warning of rockburst development processes in tunnels," *Rock Mechanics and Rock Engineering*, vol. 48, no. 5, pp. 2061–2076, 2015.

[8] Y. Yu, D. C. Zhao, G. L. Feng, D. X. Geng, and H. S. Guo, "Energy evolution and acoustic emission characteristics of uniaxial compression failure of anchored layered sandstone," *Frontiers in Earth Science*, vol. 10, p. 841598, 2022.

[9] G. L. Feng, B. R. Chen, Y. X. Xiao et al., "Microseismic characteristics of rockburst development in deep TBM tunnels with alternating soft-hard strata and application to rockburst warning: a case study of the Neelum-Jhelum hydropower project," *Tunnelling and Underground Space Technology*, vol. 122, p. 104398, 2022.

[10] B. Diezma-Iglesias, M. Ruiz-Altisent, and P. Barreiro, "Detection of internal quality in seedless watermelon by acoustic impulse response," *Biosystems Engineering*, vol. 88, no. 2, pp. 221–230, 2004.

[11] B. Diezma-Iglesias, M. Ruiz-Altisent, and P. Jancsók, "Vibrational analysis of seedless watermelons: use in the detection of internal hollows," *Spanish Journal of Agricultural Research*, vol. 3, no. 1, pp. 52–60, 2005.

[12] J. J. Burred, A. Röbel, and T. Sikora, "Polyphonic musical instrument recognition based on a dynamic model of the spectral envelope," in *2009 IEEE International Conference on Acoustics, Speech and Signal Processing*, pp. 173–176, Taipei, Taiwan, April 2009.

[13] A. Raman and A. L. Robert, "An efficient code for environmental sound classification," *The Journal of the Acoustical Society of America*, vol. 126, no. 1, pp. 7–10, 2019.

[14] D. Krijanders, M. E. Niessen, and T. C. Andringa, "Soundscape annotation and environmental source recognition experiments in Assen," in *Internoise*, Ottawa Canada, August 2009.

[15] W. Na and C. H. E. N. Ke'an, "Regression model of timbre attribute for underwater noise and its application to target recognition," *Acta Physica Sinica*, vol. 59, no. 4, pp. 2873–2881, 2010.

[16] C. Ke'an, M. Miao, and Z. Yan-ni, "Evaluation and analysis of auditory attributes for vehicle noise on Chinese expressions," *Acta Acoustica Sinica*, vol. 33, no. 4, pp. 348–353, 2008, (in Chinese).

[17] N. Wang, K. A. Chen, and H. Huang, "Subjective evaluation and analysis of auditory attributes for underwater noise," *Acta Physica Sinica*, vol. 58, no. 10, pp. 7330–7338, 2009.

[18] Y. Liang, C. Keyan, and Z. Bingrui, "Feature extraction for sound source materials recognition with impact sounds," *Acta Acoustics*, vol. 41, no. 4, pp. 521–528, 2016.

[19] Z. Kai, D. Ming-ming, L. Feng, W. Yu-shuai, S. Jin-wei, and G. U. Liang, "Experimental study on terrain classification based on acoustic signa for tracked robot," *Journal of Beijing Institute of Technology*, vol. 38, no. 9, pp. 912–916, 2018.

[20] M. C. Ozkul, A. Saranli, and Y. Yazicioglu, "Acoustic surface perception from naturally occurring step sounds of a dexterous hexapod robot," *Mechanical Systems and Signal Processing*, vol. 40, no. 1, pp. 178–193, 2013.

[21] Q. Zhang, T. Liu, and Q. Li, "Roller-integrated acoustic wave detection technique for rockfill materials," *Applied Sciences-Basel*, vol. 7, no. 11, p. 1118, 2017.

[22] A. Glowacz, W. Glowacz, Z. Glowacz, and J. Kozik, "Early fault diagnosis of bearing and stator faults of the single-phase induction motor using acoustic signals," *Measurement*, vol. 113, pp. 1–9, 2017.

[23] A. Glowacz, "Acoustic based fault diagnosis of three-phase induction motor," *Applied acoustics*, vol. 137, pp. 82–89, 2018.

[24] J. Prawin, "Breathing crack damage diagnostic strategy using improved MFCC features," *Journal of Intelligent Material Systems and Structures*, vol. 32, no. 20, pp. 2437–2462, 2021.

[25] J. S. Seo, M. Jin, S. Lee, D. Jang, S. Lee, and C. D. Yoo, "Audio fingerprinting based normalized spectral subband centroids," *Pennsylvania USA: IEEE Signal Processing SocietyProceedings.(ICASSP'05). IEEE International Conference on Acoustics, Speech, and Signal Processing*, pp. 213–216, Philadelphia, PA, March 2005.

[26] G. Lu, "A technique towards automatic audio classification and retrieval," in *Proceedings of the Fourth International Conference on Signal Processing*, pp. 1142–1145, Beijing, China, 1998.